Electronic Supplementary Material (ESI) for ChemComm.

Supporting Information

A Cationic *fcu*-Lanthanide MOF Enhances the Uptake of Iodine Vapour at Room Temperature

Clara Zwanziger,[a‡] Walace D. do Pim,[a‡] Alexandros A. Kitos,[a] Jeffrey S. Ovens,[a] Peter J. Pallister,[a] and Muralee Murugesu*[a]

[a]Department of Chemistry and Biomolecular Sciences and Centre for Catalysis Research and Innovation, University of Ottawa, Ottawa, Ontario K1N 6N5, Canada.

Table of Contents

1. Experimental Details

General Procedures

All manipulations were performed under aerobic conditions using materials as received from commercial suppliers (Alfa Aesar, TCI, and Sigma Aldrich). The ligand 4-(4'-carboxyphenyl)-1,2,4-triazole (Hcpt) was prepared according to a previously published procedure.[1]

Infrared Spectroscopy

Fourier transform infrared (FTIR) spectra were recorded using a Nicolet 6700 FT-IR spectrometer equipped with an attenuated total reflectance accessory (ATR) in the 4000-600 cm^{-1} range using 16 scans with a resolution of 4 cm^{-1}.

Powder X-ray Diffraction

PXRD patterns for bulk samples were recorded using a Rigaku Ultima IV X-ray powder diffractometer. The Bragg-Brentano geometry using Cu-Kα was employed to collect the data (λ = 1.541836 Å) in the 2θ range 5-40° at 23 °C.

Single Crystal X-ray Diffraction

Crystallographic data were collected from single crystals mounted on MiTeGen dual thickness MicroMounts using Parabar oil. Data were collected on a Bruker ApexII single crystal diffractometer equipped with a graphite monochromator. The instrument was equipped with a sealed tube Mo Kα source (λ= 0.71073 Å), an ApexII CCD detector and a dry compressed air-cooling system. All samples were cooled to approximately 200 K during data collection. Raw data collection and processing were performed with the Apex3 software package from Bruker.[2] Initial unit cell parameters were determined from 36 data frames from select ω scans. Semi-empirical absorption corrections based on equivalent reflections were applied.[3] Systematic absences in the diffraction dataset and unit cell parameters were consistent with the assigned space group. The initial structural solutions were determined using SHELXT direct methods,[4] and refined with full-matrix least-squares procedures based on F^2 using SHELXL or ShelXle.[5]. Hydrogen atoms were placed geometrically and refined using a riding model. Solvent molecules located in the voids could not be modelled explicitly, thus Platon Squeeze was used to account for this electron density.[6]

Thermogravimetric Analyses

TGA curves were collected on a TA Instruments Q5000 TGA analyzer from room temperature to 800 °C in a nitrogen atmosphere (25 mL min^{-1}), with a heating rate of 10 °C min^{-1}.

Scanning Electron Microscopy

SEM images of **Dy-UiO-66** were collected on a JEOL JSM-7500F field emission scanning electron microscope. The sample was dried in air and then mounted on carbon tape and coated with gold (6 nm). Energy-dispersive X-ray spectrum (EDS) were acquired using the Oxford Instrument EDS system.

Solid-state ^{19}F NMR

^{19}F NMR experiments were performed at 4.7 T (ν_0(1H) = 200.1 MHz) on a Bruker Avance III spectrometer. Spectra were obtained using a Bruker 2.5 mm 1H/X probe designed for a 500 MHz spectrometer. ^{19}F (ν_0 = 188.2 MHz) data were collected on the X channel of the probe but the 1H channel of the preamplifier/spectrometer. No external RF filters were used. ^{19}F MAS spectra were collected at room temperature with a spinning rate of 25 kHz in 2.5 mm zirconia rotors using a rotor-synchronized Hahn echo. A 6.5 µs 90° ^{19}F pulse was used with an echo delay of 150.25 µs which corresponds to 4 rotor cycles. A relaxation delay of 5 seconds was used, and total acquisition times ranged from 20 min to 1 h. Chemical shifts were referenced to Teflon at –122 ppm.

Gas Adsorption Studies

N_2 adsorption-desorption Isotherms were collected at 77.3 K between 0 and 1 bar using a Micromeritics 3Flex. Prior to measurements, samples were activated using a Micromeritics Smart VacPrep. The activation of **Dy-UOTT-4** and **Dy-UiO-66** have been performed by heating roughly 15 mg of samples under vacuum at 80 °C for 24 h. Specific surface areas were determined using the Brunauer−Emmett−Teller (BET), and pore size distribution (PSD) were determined by using the nonlocal density functional theory (NLDFT) method.

Inductively Coupled Plasma – Optical Emission Spectroscopy

ICP-OES analyses were performed on an Agilent ICP-OES instrument. Evacuated samples of MOFs were digested in a mixture of 0.2 mL HNO_3 and 0.6 mL HCl (**Dy-UOTT-4**) and 0.75 mL H_2SO_4 (**Dy-UiO-66**). All samples were then heated over 24 h to ensure full digestion of the sample. The solutions were then diluted to 10 mL using distilled water, and prior to measurement, they were again diluted 10x for the correct range of measurement.

Syntheses of MOFs

$[RE_6(\mu_3\text{-}F)_x(\mu_3\text{-}OH)_{8-x}(cpt)_6(EtOH)_6]$ $(NO_3)_4$ (x = 1-8) (***UOTT-4**, RE = Dy or Y).* Taking **Dy-UOTT-4** as an example, $Dy(NO_3)_3{\cdot}xH_2O$ (57 mg 0.130 mmol, assuming hexahydrate), Hcpt (49.6 mg, 0.261 mmol), and 2-fluorobenzoic acid (146.1 mg, 1.044 mmol) were combined in a 20 mL microwave vial with 1.5 mL ethanol 95% and 1 mL DMF. The vial was sealed and sonicated for 10 min then placed in an oven and heated at 120 °C for 96 h and cooled slowly to room temperature over 55 h. The afforded single crystals were washed with ethanol three times over 72 h, exchanging the solvent each 24 h. The crystals were dried under air for 1 h giving ~29% yields (15 to 20 mg). Dy calc.: 35.07%; Exp. (ICP-OES): 36.41%.

*$(NH_2Me_2)_2[Dy_6(\mu_3\text{-}F)_x(\mu_3\text{-}OH)_{8-x}(BDC)_6$ (x = 1-8) (**Dy-UiO-66**).* Preparation of this material has been adapted from a previously reported procedure for other RE-UiO-66 analogues.[7] Briefly, $Dy(NO_3)_3 \cdot 6H_2O$ (76.3 mg, 0.174 mmol), H_2BDC (28.5 mg, 0.171 mmol) and 2,6-diflurorbenzoic acid (440 mg, 2.78 mmol) were combined in a 20 mL scintillation vial along with 8 mL DMF. The vial was capped and sonicated for 10 min then set in an oven and heated at 120 °C for 96 h and cooled to room temperature over 55 h. The polycrystalline product was washed with DMF three times over the course of 72 h, exchanging the solvent each 24 h. The off-white solid was dried under air for 1 h giving ~ 44% yields (15-20 mg). Dy calc.: 44.24%; Exp. (ICP-OES): 45.63%.

The Y-UiO-66 analogue was synthesized following a previously published procedure for probing the of ^{19}F environment through solid-state NMR.[7]

Iodine Uptake Studies

In a 100 mL glass bottle, 250 mg of solid iodine was added. Separately, to three 5 mL vials, 5 mg of MOF was added, noting both the mass of the empty vial and the vial containing the sample. The three sample vials were then added to the 100 mL flask which was then sealed with parafilm, and a timer started. At each time point, the 100 mL flask was opened, the 5 mL vials removed and weighed, then they were re-added to the iodine atmosphere and the system sealed again. This procedure was done for both the activated and non-activated samples.

Scheme S1. Scheme of iodine uptake experiments, solid iodine was sealed in a glass bottle with dry MOF samples contained in a second smaller vial such that the MOF is only in contact with iodine vapours.

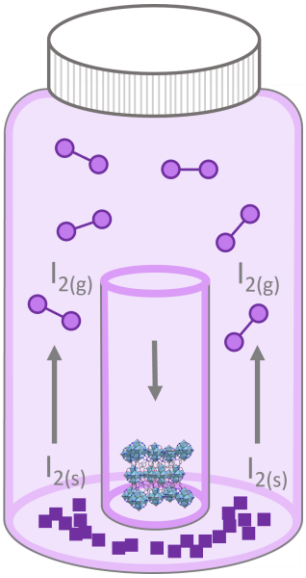

2. UOTT-4 Crystal Images

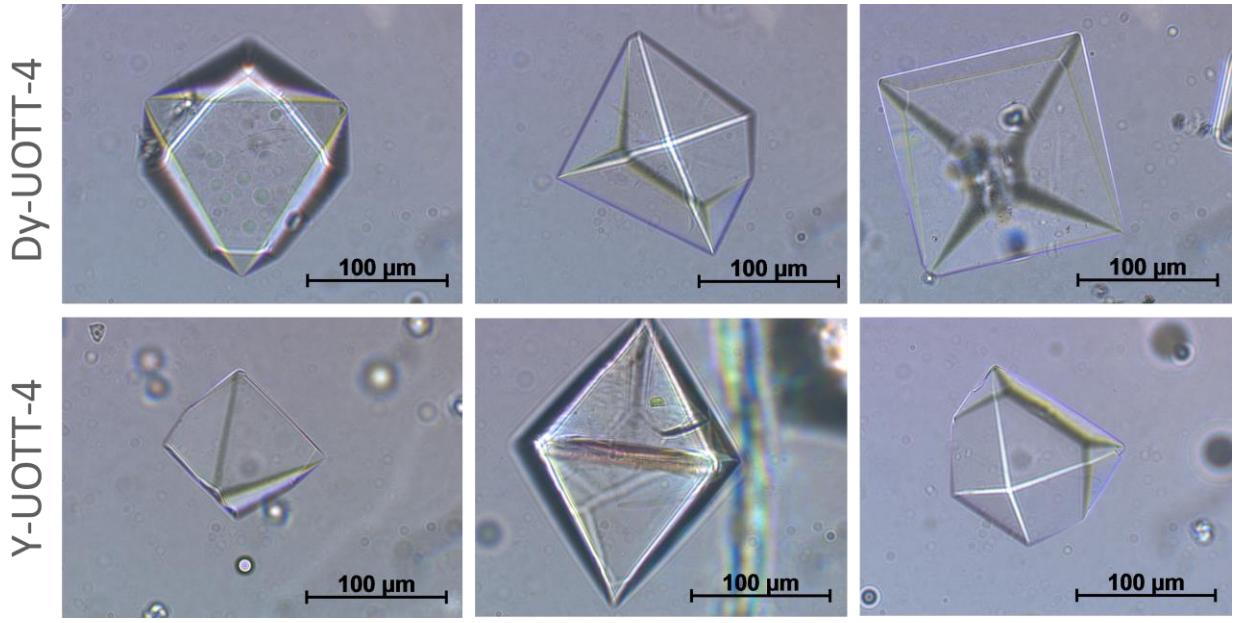

Fig. S1. Optical microscopy images of **Dy-UOTT-4** (top) and **Y-UOTT-4** (bottom) showing colorless single crystals with and octahedral shape characteristic of **fcu** topology.

3. Crystal Structure Details for Dy-UOTT-4 and Y-UOTT-4

Table S1: Crystallographic details for **Dy-UOTT-4** and **Y-UOTT-4**

	Dy-UOTT-4	**Y-UOTT-4**
CCDC number	2172076	2172077
Chemical formula	$C_{60}H_{57}Dy_6F_8N_{18}O_{18}$	$C_{60}H_{57}F_8N_{18}O_{18}Y_6$
Formula mass	2445.23	2003.69
Crystal system	Cubic	Cubic
Space group	$Fm\bar{3}m$	$Fm\bar{3}m$
a / Å	23.5185 (7)	23.4208 (7)
b / Å	23.5185 (7)	23.4208 (7)
c / Å	23.5185 (7)	23.4208 (7)
α / °	90	90
β / °	90	90
γ / °	90	90
Unit cell volume / Å^3	13008.5 (12)	12847.1 (12)
Temperature	203	208
No. of formula units/unit cell, Z	4	4
Radiation type	Mo kα, λ = 0.71073 Å	Mo kα, λ = 0.71073 Å
R_{int}	0.033	0.067
Absorption coefficient, μ / mm^{-1}	3.46	2.74
No. of reflections measured	82373	24771
No. of independent reflections	2727	1607
Final R_1 values (all data)	0.0178	0.0476
Final $wR_2(F^2)$ values (all data)	0.0450	0.0900
Final R_1 values ($I > 2\sigma(I)$)	0.0145	0.0311
Final $wR_2(F^2)$ values ($I > 2\sigma(I)$)	0.0422	0.0837
Goodness of fit on F^2	1.015	1.077

4. Shape Analysis of RE(III) in RE-UOTT-4

Table S2. Shape analysis of Dy(III) in **Dy-UOTT-4**

Code	Label	Shape	Symmetry	CShM
DyN_4F_4O				
1	EP-9	Enneagon	D_{9h}	36.630
2	OPY-9	Octagonal pyramid	C_{8v}	20.306
3	HBPY-9	Heptagonal bipyramid	D_{7h}	20.733
4	JTC-9	Johnson triangular cupola J3	C_{3v}	17.745
5	JCCU-9	Capped cube J8	C_{4v}	12.892
6	CCU-9	Spherical-relaxed capped cube	C_{4v}	10.490
7	JCSAPR-9	Capped square antiprism J10	C_{4v}	2.858
8	CSAPR-9	Spherical capped square antiprism	C_{4v}	0.768
9	JTCTPR-9	Tricapped trigonal prism J51	D_{3h}	4.295
10	TCTPR-9	Spherical tricapped trigonal prism	D_{3h}	1.777
11	JTDIC-9	Tridiminished icosahedron J63	C_{3v}	13.647
12	HH-9	Hula-hoop	C_{2v}	13.291
13	MFF-9	Muffin	C_s	0.962

Table S3. Shape analysis of Y(III) in **Y-UOTT-4**

Code	Label	Shape	Symmetry	CShM
YN_4F_4O				
1	EP-9	Enneagon	D_{9h}	36.634
2	OPY-9	Octagonal pyramid	C_{8v}	20.610
3	HBPY-9	Heptagonal bipyramid	D_{7h}	20.513
4	JTC-9	Johnson triangular cupola J3	C_{3v}	17.617
5	JCCU-9	Capped cube J8	C_{4v}	12.811
6	CCU-9	Spherical-relaxed capped cube	C_{4v}	10.413
7	JCSAPR-9	Capped square antiprism J10	C_{4v}	2.832
8	CSAPR-9	Spherical capped square antiprism	C_{4v}	0.739
9	JTCTPR-9	Tricapped trigonal prism J51	D_{3h}	4.290
10	TCTPR-9	Spherical tricapped trigonal prism	D_{3h}	1.770
11	JTDIC-9	Tridiminished icosahedron J63	C_{3v}	13.631
12	HH-9	Hula-hoop	C_{2v}	13.235
13	MFF-9	Muffin	C_s	0.886

5. Selected Bond Distances and Angles around RE(III) in RE-UOTT-4

Table S4. Selected bond distances and angles around Dy1 in **Dy-UOTT-4**, and Y1 in **Y-UOTT-4**. Symmetry codes: (i) = z,x,y; (ii) = z,x,1-y; (iii) = x,z,1-z; (iv) = x,z,y; (v) = x,1-z,y' (vi) = x,y,1-z.

Dy-UOTT-4		Y-UOTT-4	
Bond Lengths			
Bond	Length (Å)	Bond	Length (Å)
Dy1 - F1	2.33	Y1 - F1	2.31
Dy1 - F1^{i}	2.33	Y1 -F1^{i}	2.31
Dy1 - F1^{ii}	2.33	Y1 -F1^{ii}	2.31
Dy1 - F1^{iii}	2.33	Y1 -F1^{iii}	2.31
Dy1 - O1	2.33	Y1 - O1	2.30
Dy1 - O1^{iv}	2.33	Y1 - O1^{iv}	2.30
Dy1 - O1^{v}	2.33	Y1 - O1^{vi}	2.30
Dy1 - O1^{vi}	2.33	Y1 - O1^{vi}	2.30
Dy1 - O3	2.39	Y1 - O3	2.36
Dy1 - N1	2.55	Y1 - N1	2.54
Dy1 - N1^{iv}	2.55	Y1 - N1^{iv}	2.54
Dy1 -N1^{v}	2.55	Y1 - N1^{v}	2.54
Dy1 - N1^{vi}	2.55	Y1 - N1^{vi}	2.54
Bond Angles			
Entry	Angle (°)	Entry	Angle (°)
N1^{vi} - Dy1 - N1	149.80	N1^{vi} - Y1 - N1	148.60
N1^{iv} - Dy1 - N1	86.11	N1^{iv} - Y1 - N1	85.80
F1^{i} - Dy1 - F1	99.88	F1^{i} - Y1 - F1	100.06
F1 - Dy1 - F1^{ii}	65.53	F1 - Y1 - F1^{ii}	65.63
F1 - Dy1 - N1	69.21	F1 - Y1 - N1	69.64
F1 - Dy1 - O3	130.06	F1 - Y1 - O3	129.97
F1 - Dy1 - O1	76.34	F1 - Y1 - O1	76.64
N1 - Dy1 - O3	74.90	N1 - Y1 - O3	74.23
N1 - Dy1 - O1^{iv}	83.98	N1 - Y1 - O1^{iv}	83.63
N1 - Dy1 - O1^{vi}	141.15	N1 - Y1 - O1^{vi}	140.10
O3 - Dy1 - O1	66.25	O3 - Y1 - O1	65.81

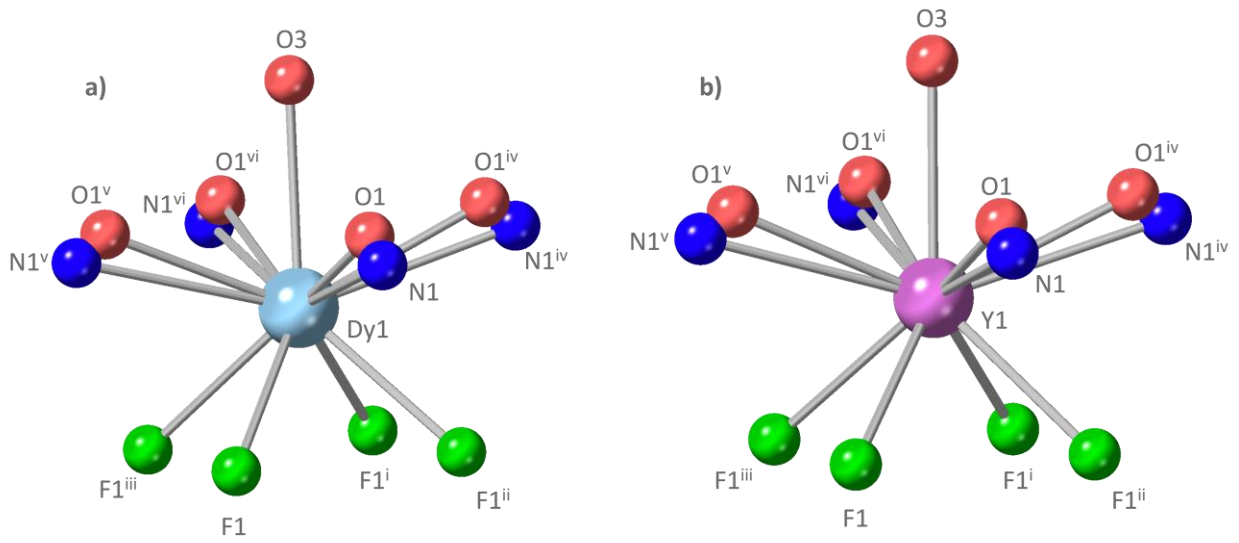

Fig. S2. Coordination environment around a) Dy1 in **Dy-UOTT-4** and b) Y1 in **Y-UOTT-4**, the disorder in the orientation of cpt linker is shown as both N1 and O1 coordinated. Symmetry codes: (i) = z,x,y; (ii) = z,x,1-y; (iii) = x,z,1-z; (iv) = x,z,y; (v) = x,1-z,y' (vi) = x,y,1-z.

6. Solid-state NMR

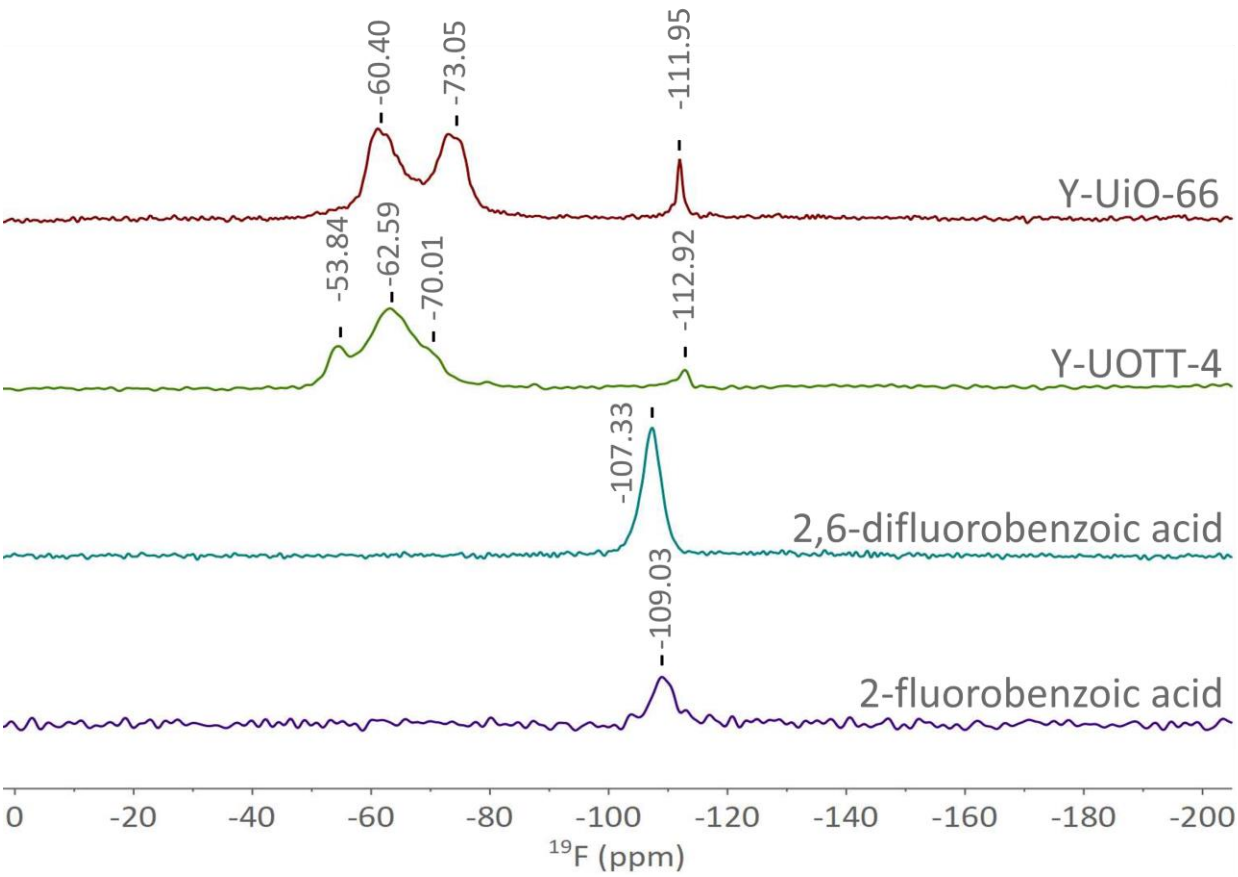

Fig. S3. Solid-state MAS ^{19}F NMR of **Y-UiO-66**, **Y-UOTT-4**, 2,6-difluorobenzoic acid, 2-fluorobenzoic acid. Spinning speed was 25 kHz.

7. SEM-EDS Analyses

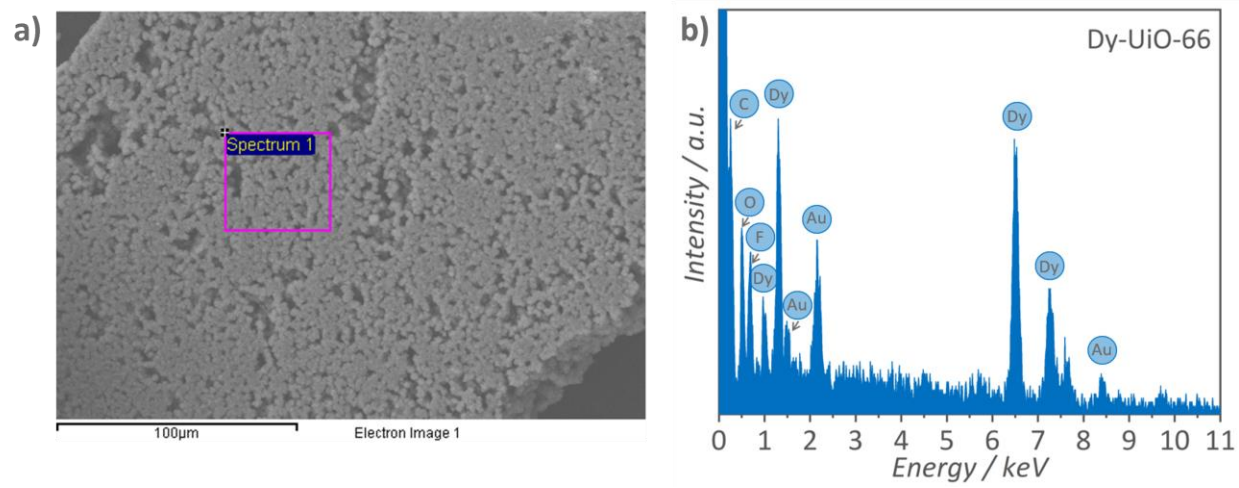

Fig. S4. SEM-EDS analyses for **Dy-UiO-66**. a) Region from the SEM image (a) which the EDS spectrum (b) was recorded; the presence Au is a result of the gold coating.

8. TGA

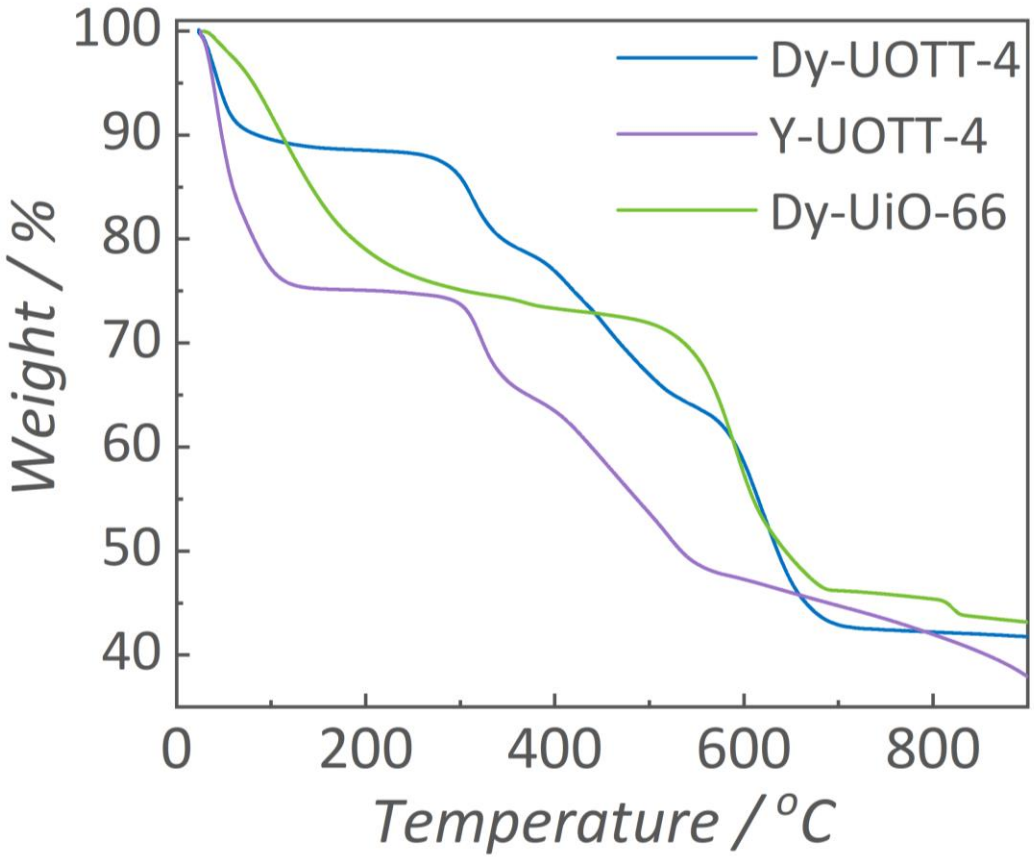

Fig. S5. Thermogravimetric analysis of **Dy-UOTT-4**, **Y-UOTT-4**, and **Dy-UiO-66**. Samples were dried in air before the analysis. The initial mass loss events are attributed to the loss of contained solvents.

9. Stability Test of Dy-UOTT-4 Using PXRD Analysis

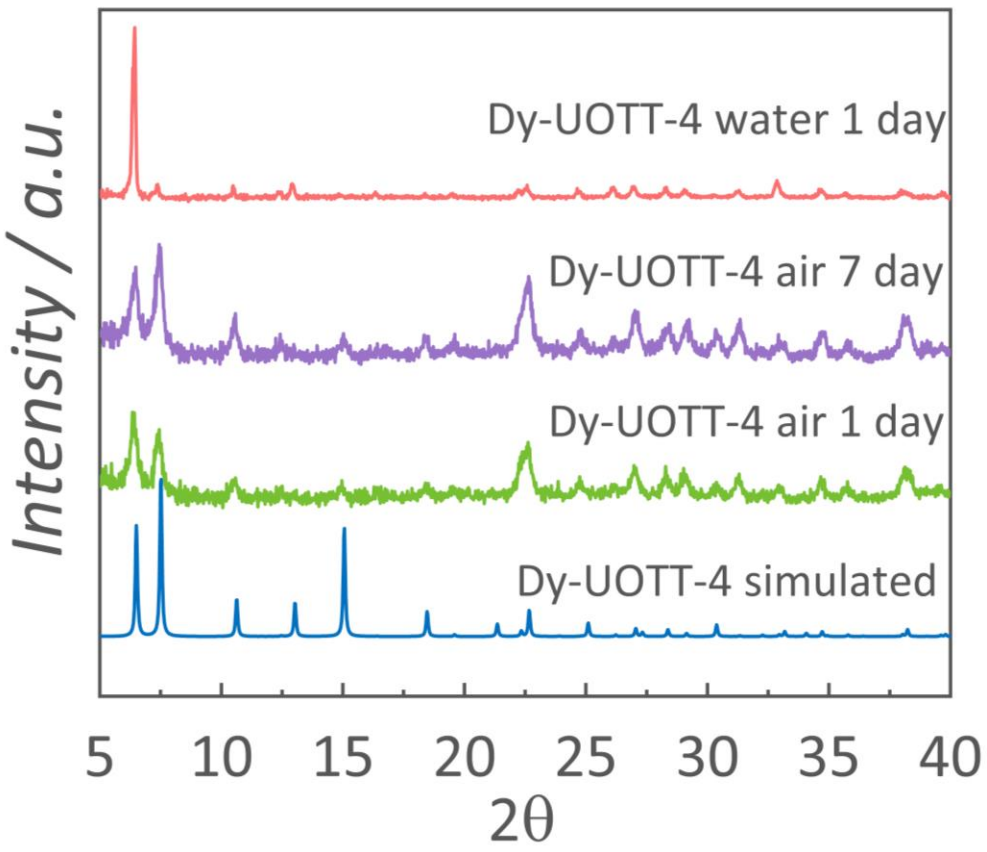

Fig. S6. PXRD patterns of **Dy-UOTT-4** following exposure to water or air, showing that crystallinity is maintained following exposure to air even after 7 days. Crystallinity is also retained after exposure to water for 1 day.

10. BET Fittings of UOTT-4 and RE-UiO-66

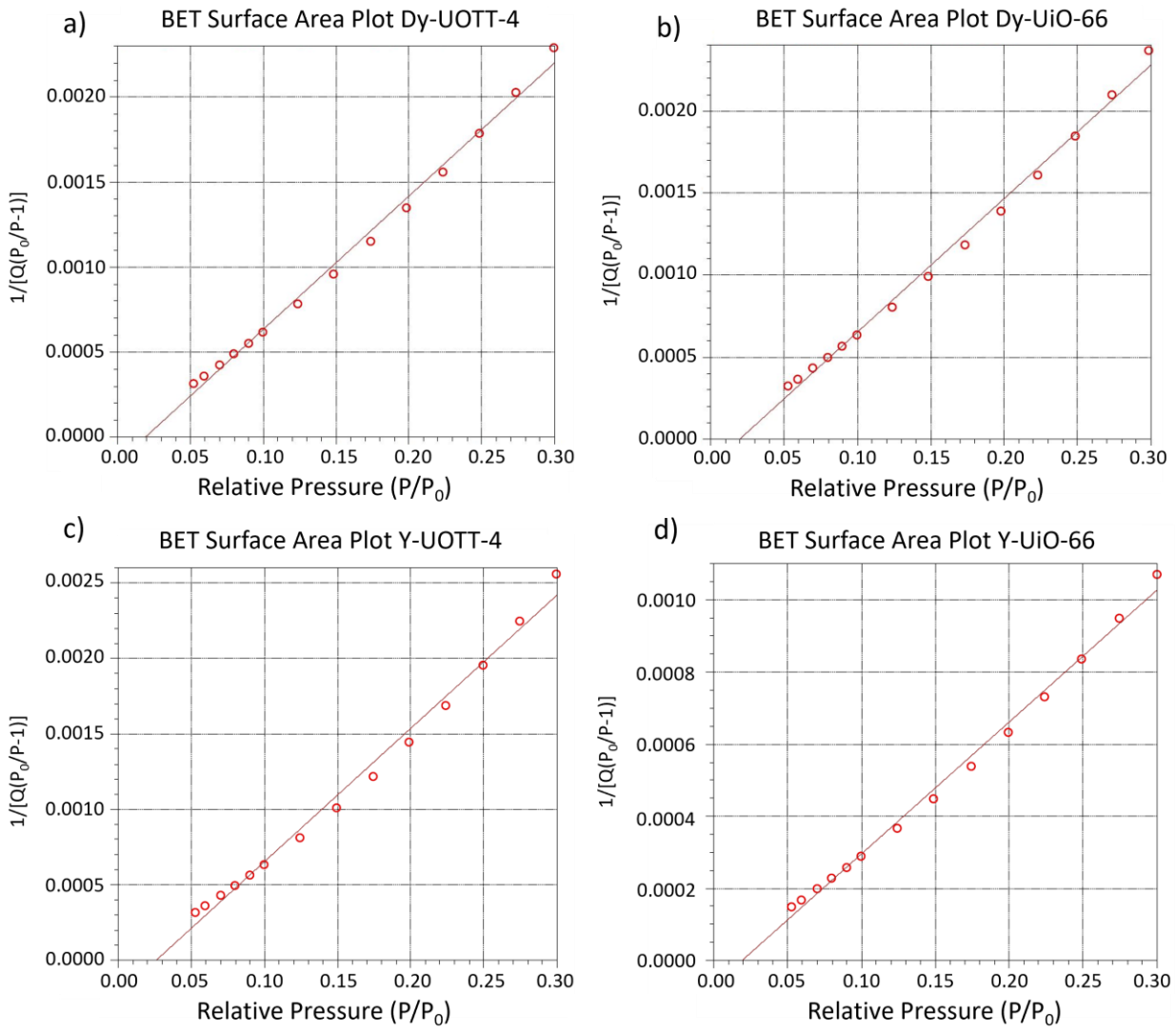

Fig. S7. Brunauer-Emmett-Teller surface area fitting of a) **Dy-UOTT-4**, S_{BET} = 566 $m^2\ g^{-1}$ b) **Dy-UiO-66**, S_{BET} = 546 $m^2\ g^{-1}$ c) **Y-UOTT-4**, S_{BET} = 506 $m^2\ g^{-1}$ d) **Y-UiO-66**, S_{BET} = 1213 $m^2\ g^{-1}$.

11. Iodine Uptake Images in Dy-UOTT-4

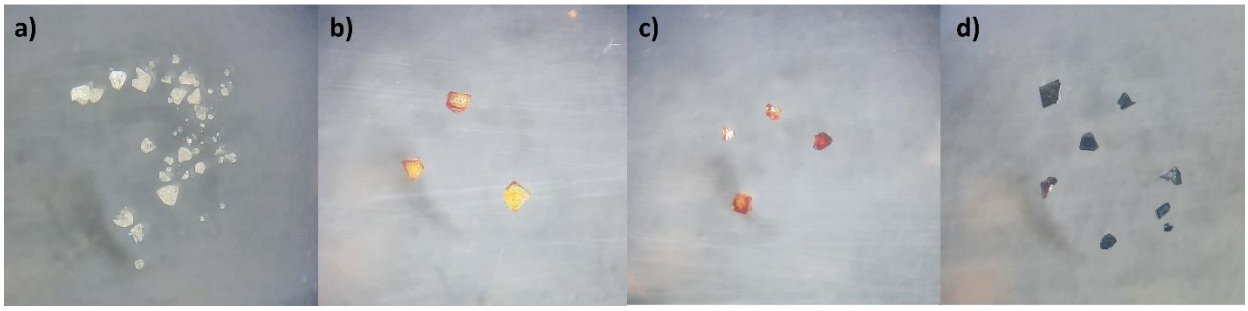

Fig. S8. Optical microscopy images of **Dy-UOTT-4** following a) 0 h, b) 3 h, c) 6 h, d) 24 h exposure to iodine vapour.

12. Iodine Adsorption Capacities of Selected MOFs

Table S5: Iodine adsorption capacities of selected MOFs.

MOF	BET surface area ($m^2\ g^{-1}$)	Pore volume ($cm^3\ g^{-1}$)	Iodine uptake ($g\ g^{-1}$)	Temperature (^oC)	Ref.
Dy-UOTT-4	**566**	**0.25**	**0.40**	**23 ^oC**	**This work**
Dy-UiO-66	**546**	**0.24**	**0.15**	**23 ^oC**	**This work**
UiO-66	1072	0.53	0.66	80 ^oC	8
UiO-67	2638	1.17	0.53	80 ^oC	8
ZIF-8	1630	0.66	1.25	77 ^oC	9
SION-8	509	—	0.46	25 ^oC	10
MOF-808	1930	0.82	2.18	80 ^oC	8
NU-1000	2126	1.27	1.45	80 ^oC	8
MOF-867	2403	1.12	0.88	80 ^oC	8
MFM-300(In)	1050	0.41	1.16	80 ^oC	11
MFM-300(Sc)	1250	0.50	1.54	80 ^oC	11
MFM-300(Fe)	1192	0.46	1.29	80 ^oC	11
MFM-300(Al)	1370	0.37	0.94	80 ^oC	11
Th-SINAP-13	3396	—	0.60	75 ^oC	12
HKUST-1	1850	0.74	1.75	75 ^oC	13

13. Iodine Uptake in Y-UiO-66

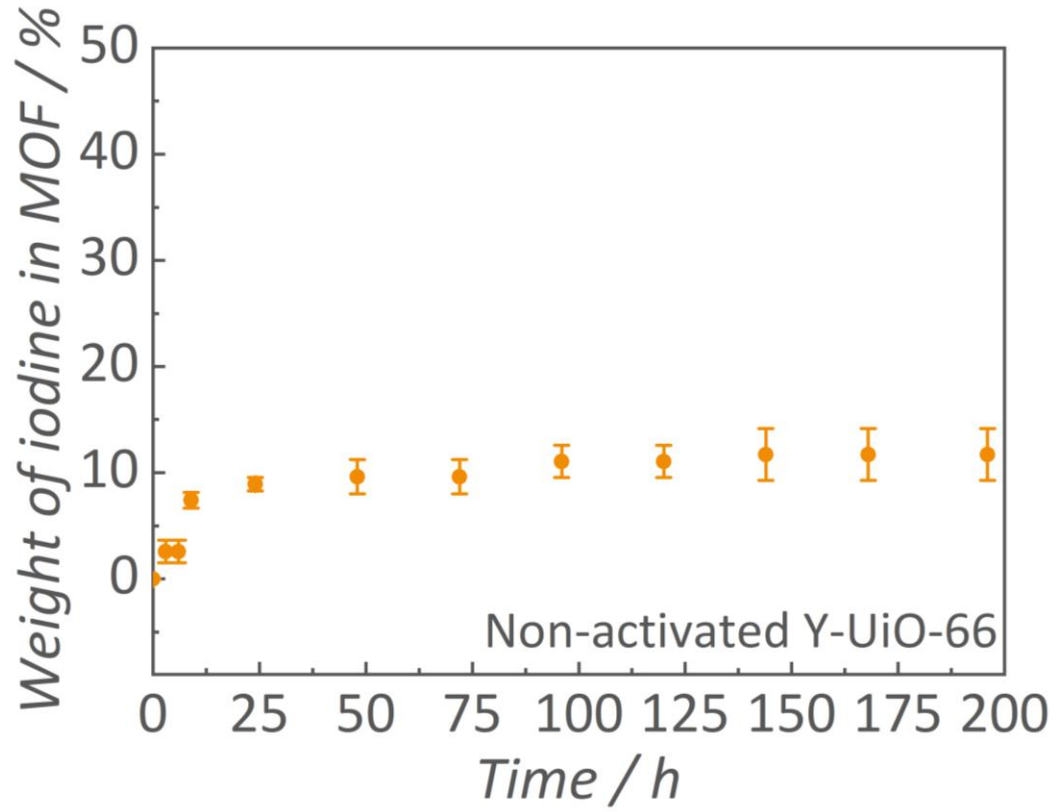

Fig. S9. Gravimetric uptake of iodine vapours at ambient temperature (23 °C) in non-activated **Y-UiO-66**. Uncertainty in data points was determined through standard deviation of triplicate experiments.

14. FTIR spectra

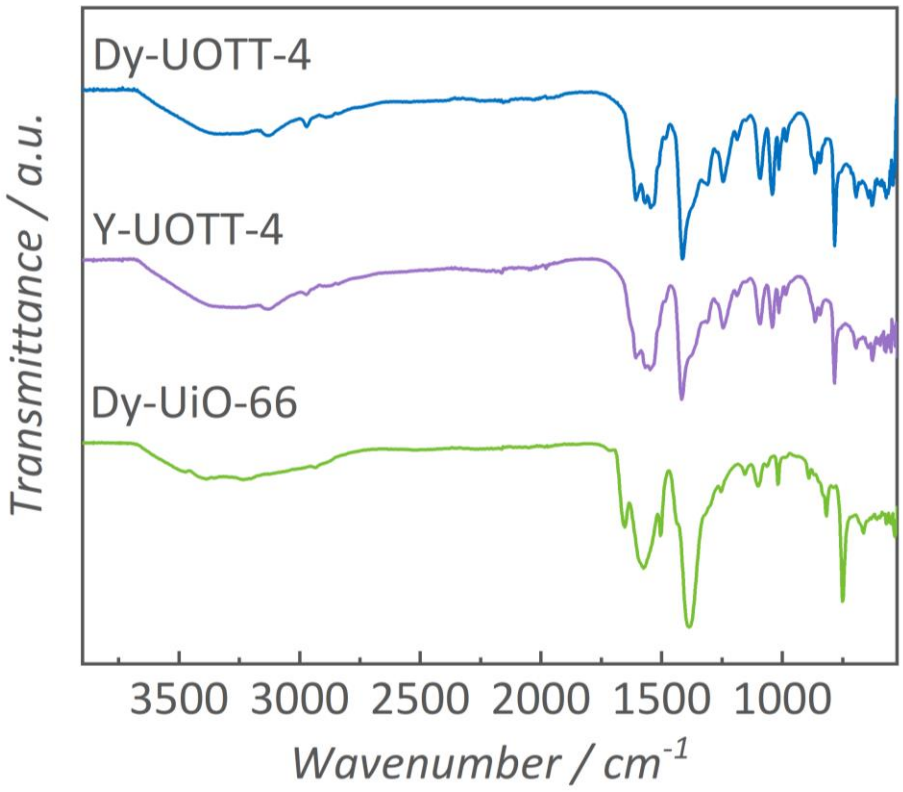

Fig S10. FTIR spectra of **RE-UOTT-4** (RE = Dy and Y) and **Dy-UiO-66**.

15. ICP-OES analyses

Table S6: Theoretical %Dy in **Dy-UOTT-4** and **Dy-UiO-66** compared to experimental results from ICP-OES measurements.

Sample	% RE calculated	% RE ICP-OES
Dy-UOTT-4	35.07	36.41
Dy-UiO-66	44.24	45.63

16. References

1 T. Aharen, F. Habib, I. Korobkov, T. J. Burchell, R. Guillet-Nicolas, F. Kleiz, M. Murugesu, *Dalton Trans.,* 2013, **42**, 7795.

2 APEX Softward Suite. Bruker AXS Inc: Madison Wisconsin USA, 2010.

3 R. H. Blessing, *Acta Crystallogr. A,* 1995, **51**, 33–38.

4 G. M. Sheldrick, *Acta Crystallogr. A,* 2008, **64**, 112–122.

5 C.B. Hübschle, G. M. Sheldrick, B. Dittrich, ShelXle: A Qt Graphical User Interface for SHELXL. *J. Appl. Crystallogr.,* 2011, **44**, 1281–1284.

6 A. L. Spec, *Acta Crystallogr., Sect. C: Struct. Chem.*, 2015, **71**, 9–18.

7 P. R. Donnarumma, S. Frojmovic, P. Marino, H. A. Bicalho, H. M. Titi and A. J. Howarth, *Chem. Commun.*, 2021, **57**, 6121–6124.

8 P. Chen, X. He, M. Pang, X. Dong, S. Zhao and W. Zhang, *ACS Appl. Mater. Interfaces*, 2020, **12**, 20429—20439.

9 D. F. Sava, M. A. Rodriguez, K. W. Chapman, P. J. Chupas, J. A. Greathouse, P. S. Crozier and T. M. Nenoff, *J. Am. Chem. Soc.* 2011, 133, **32**, 12398—12401.

10 A. Gładysiak, T. N. Nguyen, M. Spodaryk, J. H. Lee, J. B. Neaton, A. Züttel and K. C. Stylianou, *Chem. –Eur. J.*, 2019, **25**, 501—506.

11 X. Zhang, I. Da Silva, H. G. W. Godfrey, S. K. Callear, S. A. Sapchenko, Y. Cheng, I. Vitórica-Yrezábal, M. D. Frogley, G. Cinque, C. C. Tang, C. Giacobbe, C. Dejoie, S. Rudić, A. J. Ramirez-Cuesta, M. A. Denecke, S. Yang and M. Schröder, *J. Am. Chem. Soc.*, 2017, **139**, 16289—16296.

12 Z. J. Li, Y. Ju, Y. Ju, B. Yu, X. Wu, H. Lu, Y. Li, J. Zhou, X. Guo, Z. H. Zhang, J. Lin, J. Q. Wang, J. Q. Wang and S. Wang, *Chem. Commun.*, 2020, **56**, 6715—6718.

13 D. F. Sava, K. W. Chapman, M. A. Rodriguez, J. A. Greathouse, P. S. Crozier, H. Zhao, P. J. Chupas and T. M. Nenoff, *Chem. Mater.* 2013, **25**, 13, 2591—2596.